

Applications of Artificial Neural Network Simulation for Prediction of Wear Rate and Coefficient of Friction Titanium Matrix Composites

K.K. Arun^a, N. Mary Jasmin^b, V.V. Kamesh^c, V.R. Pramod^d, S. Krishnaraj^e,

Vellingiri Suresh^{f*}, Ram Subbiah^g

^aKumaraguru College of Technology, Department of Mechanical Engineering, Coimbatore, India.

^bAndhra University college of engineering, Andhra University, Visakhapatnam, India.

^cAditya Engineering College, Department of Mechanical Engineering, Surampalem, India.

^dNSS College of Engineering, Department of Mechanical Engineering, Palakkad, India.

^eSri Sairam Engineering College, Department of Mechanical Engineering, Chennai, India.

^fAdhi College of Engineering and Technology, Department of Mechanical Engineering, Kanchipuram, India.

^gGokaraju Rangaraju Institute of Engineering and Technology, Department of Mechanical Engineering, Hyderabad, India.

Received: July 05, 2022; Revised: January 24, 2023; Accepted: February 01, 2023

The Artificial Neural Network (ANN) techniques were utilized to predict wear rate and CoF of the Ti-5Al-2.5Sn matrix reinforced with B₄C particle manufactured by the powder metallurgy. TMCs and wear test samples were characterized by the Scanning Electron Microscope (SEM). Dry sliding wear narrative of the composites was estimated on a pin-on-disc machine at various loads of 20-60N, sliding velocity of 2-6m/s and sliding distance from 1000m-3000m. The wear rate of the composite was reduced by augmentation in weight fraction of boron carbide from 3-9%. The benefits of interfacial TMCs with B₄C are: increase in strength, wear-resistance, and volume fraction. ANN was planned and utilizes a Levenburg-Marquardt program algorithm to reduce the mean squared error using a back-propagation technique. The input parameters are considered to include load, sliding velocity, and sliding distance. The experimental results of an ANN model and regression model are compared. ANN replicas have been urbanized to foreshow experimental rate of wear and CoF of TMCs and examined that ANN predictions have exceptional concord with deliberated values. Accordingly, the prediction of wear rate and CoF of TMCs using ANN in earlier actual manufacture will significantly save the manufacturing time, exertion, and expenditure.

Keywords: ANN, TMCs, Wear, Powder metallurgy, SEM.

1. Introduction

Titanium and its alloys have amazing physical, chemical, and mechanical characteristics such as low density, high corrosion resistance, and comparatively low elastic modulus making them more suitable for industrial, aerospace, marine, power plant, chemical, sport, and biomedical applications¹⁻⁶. TMCs possess significant mechanical characteristics, such as high specific strength, thermal stability, erosion, corrosion, and creep resistance^{7,8}.

Ti-5Al-2.5Sn gives an impressive performance and is considered as the workhorse in the titanium and alloys product manufacturing engineering since its inception in the early 1950s^{9,10}, the industry has evolved. Ti-5Al-2.5Sn alloys have exceptional weldability and are usually utilized in airframe applications, particularly on weldability of the aerospace structural constituents close to engines where they can withstand super high temperatures^{11,12}.

Ti-5Al-2.5Sn also acquires superior ductility and fracture toughness at tremendously low down temperatures whereas the prominent Ti-6Al-4V alloy It loses its ductility^{9,13,14}. Ti-5Al-2.5Sn alloy is low in cost, economics and cheaper than the well Ti-6Al-4V is an alloy. Ti-5Al-2.5Sn alloy, which formed near to and under alpha, is preferred for use in high-temperature cryogenic applications. Due to its low heat conductivity and chemical reactivity, the efficiency of machining titanium alloys is negatively influenced by early tool wear when using standard machining techniques. Rapid tool wear is a problem that needs to be solved when titanium alloys cutting¹³.

A metal matrix composite has two categories based on the form of reinforcement. The first form of reinforcement is squashy reinforcement as of graphite and the next form is of tough particulates like SiC, Al₂O₃, TiC, TiO₂, and others. The use of hard particulates minimizes loss of wear, mainly contrasting to the matrix main alloys^{15,16}. The TMCs produced

*e-mail: winsureshv2011@gmail.com

by the addition of B_4C showed a greater tensile elongation. The tensile elongation of TMCs attained with B_4C improved as the coarse reinforcements manufactured by B_4C could be more easily cracked at the fracture surface^{17,18}.

The hardness of the composites increased as compared to the base material (Ti-6Al-4V) and TMCs/10 B_4C which is accredited to the incidence of the rigid ceramic stage. ANOVA was utilized to verify the legality of the urbanized model. The optimal constraints of WR and CoF were recognized and so was abridged wear rate^{19,20}. Powder metallurgy is commonly used for the production of processed MMC materials with sufficient potential that can be used in many applications instead of obtaining a few admirable properties over other competing methods²¹.

An ANN-based replica is very critical and complex than another pragmatic modelling approach. It also necessitates significant acquaintance and knowledge to pertain efficiently and has been functioning predominantly for examining the link among input and output constraints of materials dispensation method²²⁻²⁵. ANN is an excellent pertinent technique due to its significant merits of superfluous precision, low cost, and shorter time. Recognizing every type of complex nonlinear interaction between input parameters and prediction of the output parameter is probable with ANN²⁶⁻²⁹. The complexity of ANN-based modeling is often higher than that of other empirical modeling techniques. In order to use it properly, it also requires a great deal of knowledge and expertise, and it has mostly been used to examine the relationship between the input and output parameters of materials processing processes²⁷.

The ANN and regression analysis is used in optimization of the manufacturing process and proved that ANN showed improved results³⁰⁻³⁴. An ANN technique was pertained earlier for predicting the process parameter routine in several applications^{26,27,29,31,33-35}. Mondal et al.³⁰ used Flower Pollination Algorithm (FPA)- based optimization of drilling burr using regression analysis and ANN model and concluded that ANN produced better results. Ivan I Argatova (2019) investigated the usage of the neural network as an aspect of a necessary type nonlinear regression model guided by the spatial understanding of the experimental collection of data. It was for a pedestal on a scrupulous group of investigational data for the composites showed, the efficiency of the ANN-supported Archard – Kragelsky regression model³⁶. Palanivel R (2019) examined and found the link among friction welding titanium joints by the relevance of an ANN technique. The joints were modelled by the relevance of the RSM³⁷. Ashan et al.³² studied that an ANN model was more precise as compared to RSM. Hassan et al.³¹ observed the fatigue performance of composite shafts by ANN and discussed that it forecasted predictions of superior quality. Wang et al.³⁴ utilized an ANN model to depict the bending force deeds in a hot strip rolling process. Chen et al.³³ found an ANN model for the prediction of the surface roughness of titanium alloys while making an allowance for cutting forces and tool vibrations as input parameters. IlkerKucukoglu researched artificial neural network technique, an artificial intelligence tool commonly used for identification and it was tested and evaluated. A capable ANN with a two-layer feed-forward structure has been identified in this analysis.

The ANN rating precision for the study results were 88.9% and 95.0% for all calculation details. Details of the experiments carried out for the neural network have shown that ANN is a useful and appropriate tool for identifying faulty assembly operations by the considered wearable devices³⁸.

The current research work executes the artificial neural network technique to they predict the wear rate of TMCs under different load conditions. Rahmath Ulla Baig (2020) developed and tested ANN predictions that were precise with an overall regression of 0.9993. The addition of reinforcement has augmented the wear resistance of aluminium MMC³⁹. Sosimi et al.⁴⁰, analyzed the ANN-LM model and the results showed the prediction precisely and the model provided an enhanced routine. Mutuk et al.⁴¹ observed an ANN model for predicting the wear rate values of the composite that was created. This entails that the wear rate can be predicted by the structure of ANN is predicated with good accuracy by the experimental data.

Kannaiyan and Raghuvaran⁴² analyzed the evaluation of wears of ANN modelling methods which were tested, and the performance of the model was found satisfactory. The ANN-based process was found to be the most suitable one in the calculation of performance response. Dinaharan et al.⁴³ used an ANN to foreshow the wear rate composites formed by friction stir processing (FSP). The DoE approach was utilized to direct the investigation. Pati⁴⁴ studied the ANN approach to predict used nonlinear regressive predictive equation showing the wear rate of the composites and showed improved superior wear resistance of the composite. Megahed et al.⁴⁵ examined that on augmentation of both the load and sliding distance it leads to an augment of the wear rate. The augment in the weight fraction of Al_2O_3 diminishes the wear rate appreciably. The ANN approach is a successful model for predicting the wear rate of Al-Si/ Al_2O_3 composite.

Sweety Mahanta et al.⁴⁶ performed a wear test and considered three input parameters L, D, V; to investigate WR and CoF creation of the output parameters. The investigational resultant is examined by RSM at the same time as the wear performance extrapolative model is urbanized by using ANN. Pramod et al.⁴⁷ measured wear analysis of damage to parts of the system, and, to investigate this specific phenomenon, research was conducted by using the L27 orthogonal array method. For predicting the tribological behaviour of the Al7075- Al_2O_3 composites, an ANN was developed using the Levenberg – Marquardt optimization model. Gampala Satyanarayana et al.⁴⁸ reported a mathematical regression model and ANN models were urbanized to foreshow the conjectural rate of wear rate of the Al/red mud nanocomposites and found that ANN calculation showed exceptional conformity with premeditated values than the other models. Hanief and Wani⁴⁹ formed a model for the wear analysis. ANN's findings are significantly higher than the standard model. It is manifested from the analysis that together the developed and ANN models could be used to determine where wear rate could run through with precise accuracy.

The literature survey concludes the TMCs were utilized to enhance physical, chemical, thermal, tribological and mechanical properties like that hardness, density, thermal conductivity, wear, corrosion, abrasion, erosion, tensile, compression, impact, and flexure. In generally preparations

of the composites were used stir casting, squeeze casting, die casting and powder metallurgy. The powder metallurgy is the one of the best technique to develop metal matrix composites and the ANN tool is the best predict the wear resistance.

The objective of the current investigation is to generate and utilize the ANN technique that could be associated in measuring the tribological behaviour of the Ti 5Al-2.5Sn/B₄C composites under different load, velocity, and distance conditions. An influential ANN technique is described to foresee the wear and CoF deeds of TMCs using neural network software MATLAB R2018b for the assessment and ANN outcomes be presently thought about.

2. Materials and Methods

2.1. Materials

Titanium alloy (Ti 5Al-2.5Sn) matrix material with powder mean size of 35–40 μm was considered for this experiment. Ti 5Al-2.5Sn is a non-heat immoderation able alloy that can attain superior weldability with stability. It also contains good high-temperature steadiness, high strength, superior corrosion opposes and fine creep opposes. Creep mentions the occurrence of plastic strain for longer periods of time, which ensues at high temperatures. Ti 5Al-2.5Sn is generally utilized in aircraft, airframe, and cryogenic applications⁵⁰. B₄C with an indicate size of 20–40 μm was used as reinforcement in this work for requirement for dispersal strengthening. The yield strength of TMCs with 3, 6, and 9% of the addition of B₄C is a further representation of the

believed collective effects of next phase strengthening, grain refinement, and solution strengthening. Specification of the powder details used in this work for the powder compaction process is provided in Table 1.

2.2. Preparation of composite

The powder metallurgy method was used for embryonic TMCs reinforced with B₄C made during the chemical vapor authentication process. Predominantly, the powders were weighed up in conformity with diverse compositions as Ti 5Al-2.5Sn with 3%, 6%, and 9% B₄C. The weighed proportion was then intermingled to make use of a planetary ball mill for a total of 7 hours through an interlude of 45 minutes for each and every 1 hour for the progress of dispersal of B₄C into the matrix. Scanning's of SEM of B₄C subsequent to intermingling amalgamation of powders are shown in Figure 1. These micrographs carry an obvious vision for the dispersal of B₄C in TMCs. The composite combination was then dense at 750 MPa using a hydraulic press to attain cylindrical specimens with 10 X 30 mm in diameter and height respectively. Subsequent to compacting, composite specimen as per standard measurements was sintered in the incidence of air at 950 °C for 1 hour⁵¹.

Table 1. Specification of powders.

Powder	Mean size(μm)	Purity/%	Density(g/cm ³)
Ti 5Al-2.5Sn	35–40	99	4.48
B ₄ C	20–40	99.5	2.52

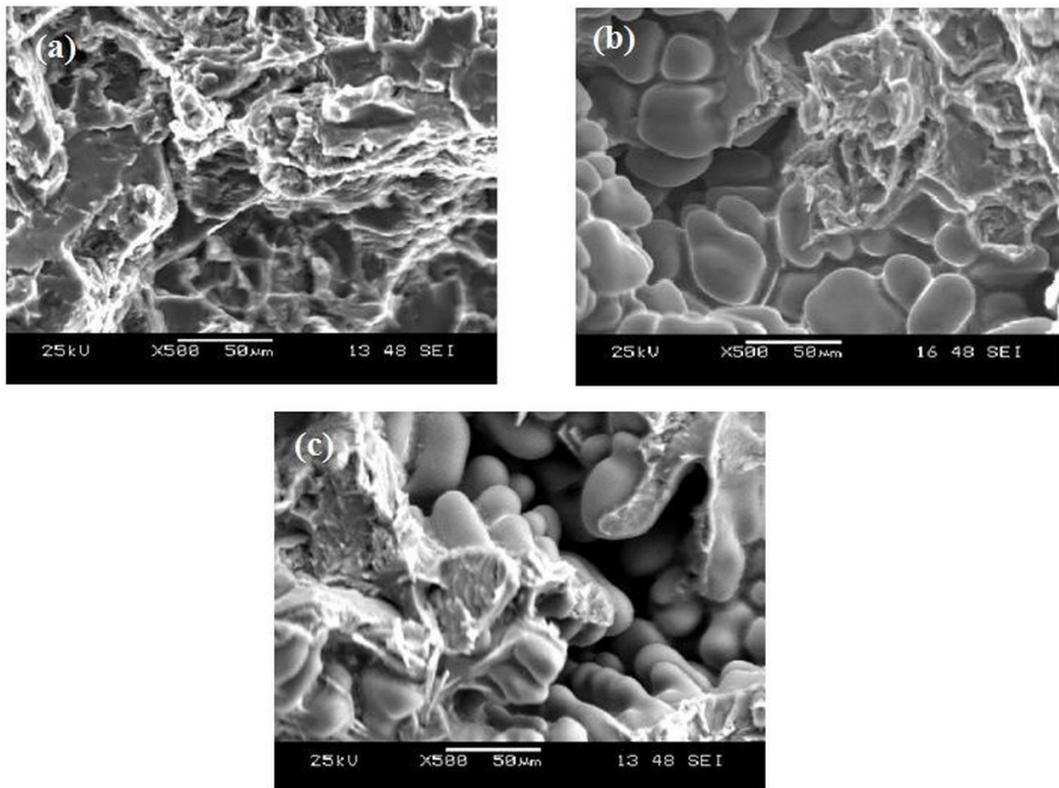


Figure 1. SEM images of TMCs (a) Ti 5Al-2.5Sn+3% B₄C (b) Ti 5Al-2.5Sn+6% B₄C and (c) Ti 5Al-2.5Sn+9% B₄C.

2.3. Microstructure of the composite

The titanium matrix composites specimens remained erudite for removing rubbish present on the surface. Particle distribution remains estimated at the support of optical microscopes. The powder metallurgy process remained inspected under the optical microscope to determine the reinforcement pattern of the powder metallurgy method. They remained grained using 100 grit silicon carbide paper tracked by 220 to 1,000 grades of emery paper ahead of optical surveillance the specimen were automatically polished and engraved by Keller's reagent to attain an improved disparity. The samples remained pictured on diverse magnifications to display the occurrence of reinforcements and its allocation of the metal matrix diverse elements/compounds which were presented in the graphite and boron carbide are difficult to distinguish by optical micrographs.

The microstructure of the Titanium matrix alloy formed by the powder metallurgy method is shown in Figure 2 The matrix particle distribution was uniform, according to microstructure analysis. The inclusion of 3%, 6%, and 9% boron carbide in this situation provides a benefit by minimizing the corrosion caused by the interaction with the titanium matrix. It was obvious that the 9% graphite interacted with the titanium matrix, causing corrosion, and that its higher volume in respect to the substrates

might enable powder to escape from the matrix and onto the reinforcement. This resulted in the reinforcement fracturing and degrading, and the strength qualities deteriorating as a result. It might be because of the creation of boron carbide as a result of the interaction between carbon and boron, which results in an increase in strength and hardness.

2.4. XRD analysis

Figure 3 displays the Ti alloy and TMCs' XRD patterns. The suggested powder metallurgy composites' phase structure was ascertained using X-ray diffraction analysis. It can be seen from Figure 4 that the suggested composite's needed composition is clear. The existence of the matrix is guaranteed by the high intensity of the Ti peak, and the difference in intensity of the B_4C phases distinguishes between variations in the weight % of composites. All composites shared the XRD phases that were discovered. These patterns demonstrate the incorporation of B_4C particles into the Ti matrix, demonstrating the suitability of the powder metallurgy process for producing B_4C reinforced TMCs.

2.5. Wear test experiment

Dry sliding wear tests for a different sample were carried out by using a pin-on-disc machine supplied by DUCOM as

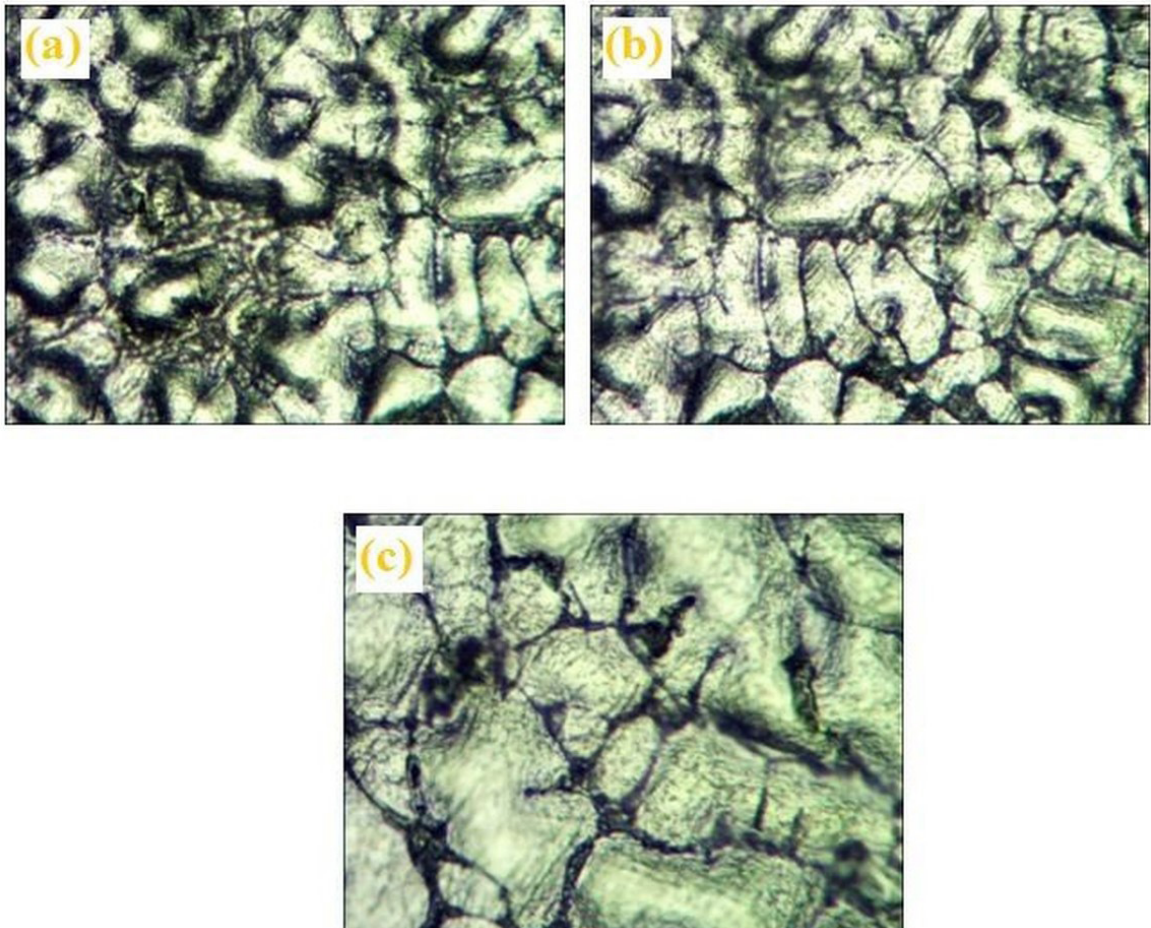


Figure 2. Optical Micrographs of TMCs (a) Ti 5Al-2.5Sn+3% B_4C (b) Ti 5Al-2.5Sn+6% B_4C and (c) Ti 5Al-2.5Sn+9% B_4C .

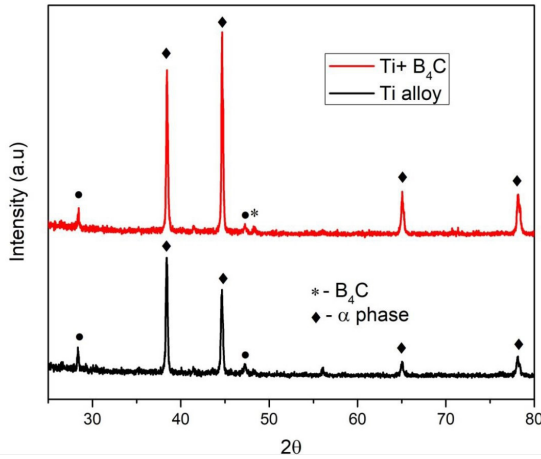


Figure 3. XRD analysis of TMCs.

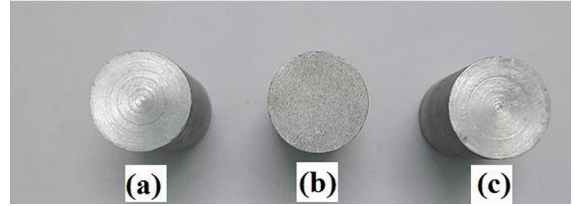


Figure 5. Wear test samples of TMCs (a) Ti 5Al-2.5Sn+3% B_4C (b) Ti 5Al-2.5Sn+6% B_4C and (c) Ti 5Al-2.5Sn+9% B_4C .

Table 2. Wear Test parameters.

Load(N)	20,40,60
Sliding velocity (m/s)	2,4,6
Sliding distance (m)	1000 to 3000
Dimension(mm)	30x10



Figure 4. Wear testing machine.

shown in Figure 4. In pin on disc wear test equipment, the disc material is grade H11 tool steel and followed ASTM G99 standard. The disc has a 500 HB hardness rating. H11 is a low carbon, high chromium, hot work tool steel with good toughness. By air quenching, this alloy has the capacity to undergo profound hardening. This alloy is suitable for severely stressed structural components in the aerospace sector because to its low carbon content and toughness. The Figure 5 shows the samples of the wear test specimen. The sample was whipped beside the counteract face of a revolving disc with a wear pathway diameter of 60 mm. The sample was loaded beside the disc during a deadweight loading system. The wear test for different specimens was carried below the normal loads of 20N, 40N, 60N, and a sliding velocity of 2, 4, and 6m/s. Wear tests were conducted

for a total sliding distance of 3000 m beneath parallel surroundings as conversed below. The wear test parameters details are shown in Table 2.

2.6. Artificial Neural Network (ANN) structure

The predictions play a vital role in modern science and technology and in this ANN play an amazing role. ANN is a physically stirred computer program designed to replicate the system in which the human natural brain processes information. ANN provides a range of powerful new techniques for solving problems in materials science and engineering applications⁵².

The predictive capabilities of ANN-based on the training on experimental data and then validated by an assortment of proper neural network structure are important. The expansion and implementation of the network model were approved by means of neural network utensils from MATLAB R2018b software⁵³. ANN architecture is one among the back-propagation method which has been working as per the flow chart shown in Figure 6.

In this investigation, ANN was shown to be working to predict the wear rate and CoF of TMCs reinforced with B_4C . The ANN network is defined to have three layers such as input, hidden, and output layer. The input layer utilized 3 parameters (L, V, D), the ten hidden layers of neurons and two outputs (WR and CoF), were speckled according to the optimum output requirement. The function of the ANN model is alienated into two significant steps such as forward computing and rearward erudition. The input parameters, pertaining to the neurons of the first layer, are meager stimuli to the network in forwarding computing step⁵⁴. The hidden neurons are associated to each other in the output layer so that change in the value of one node has an effect on the value of another⁵⁵. Figure 7 shows urbanized ANN architecture among single based buried layer. In this urbanized architecture, ANN 3 stands for the input parameter layer (L, V, D), 10 means of neurons (hidden layer) and 2 is the output parameter, b and w mentioned are for the biases and weights respectively. In Figure 7, the transfer function associated with the buried layer is Tansig and is signified by a curvature.

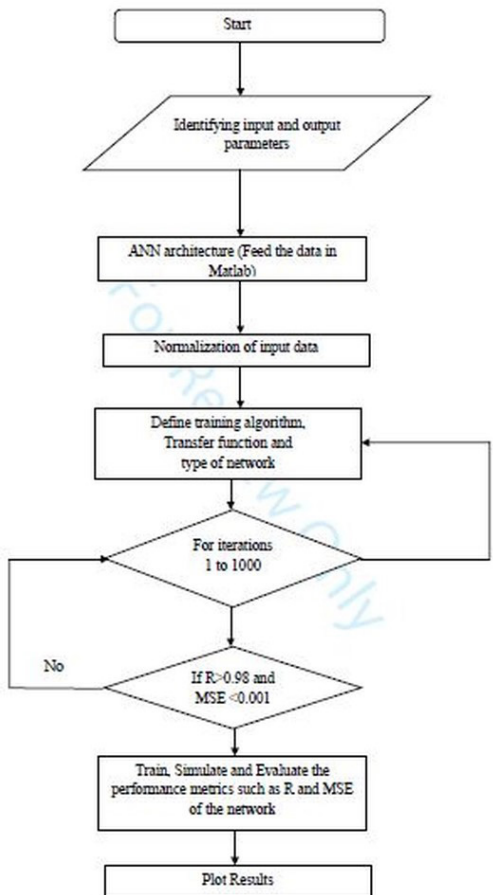


Figure 6. Flow chart of ANN architecture.

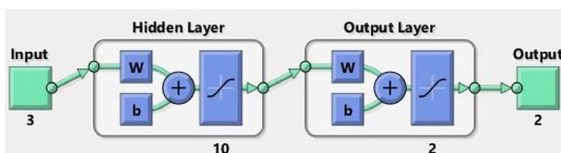


Figure 7. Representation of single concealed layer in ANN architecture.

The transfer function pure lin is used in the output layer and is shown by the appearance of a straight line. The design of experiment (L27 array) for wear of the TMCs is presented in Table 3.

3. Results and Discussion

3.1. Analysis of wear debris and worn surfaces

The investigation analysis of the wear debris and the worn surface was carried out with the help of SEM. The morphological examination of the wear wreckage confirmed the results. SEM micrographs of titanium alloy, after dry sliding wear conditions are shown in Figures 8(a), 8(b) and 8(c). Figure 8(a) shows the wear surface clearly exhibiting the presence of delaminated layers, and deep grooves. The worn surface of the TMCs clearly reveals the incidence of wear tracks, delaminated layers, and deep grooves. The layer has

Table 3. The design of experiment (L27 array).

S.No.	Load (L) N	Sliding velocity (V) (m/s)	Sliding distance (D) (m)
1.	1	1	1
2.	1	1	1
3.	1	1	1
4.	1	2	2
5.	1	2	2
6.	1	2	2
7.	1	3	3
8.	1	3	3
9.	1	3	3
10.	2	1	2
11.	2	1	2
12.	2	1	2
13.	2	2	3
14.	2	2	3
15.	2	2	3
16.	2	3	1
17.	2	3	1
18.	2	3	1
19.	3	1	3
20.	3	1	3
21.	3	1	3
22.	3	2	1
23.	3	2	1
24.	3	2	1
25.	3	3	2
26.	3	3	2
27.	3	3	2

stimulated the sliding surface clearly, as shown in Figure 8(a). The surfaces also appear to be smooth because of the boron reinforcement content and the incidence of deep grooves, which may have augmented the wear loss. The surface of the TMCs (Figure 8(b)) apparently reveals the incidence of delaminated layers and debris, observation shows the occurrence of debris and wrecked particles. The surface of the TMCs (Figure 8(c)) visibly exposes the prevalence of cracks, delamination, and deep grooves. Imprecise grooves and fine grazes were created on the worn surface. The wear mechanisms are disposition by the arrangement of the undulation, which is fashioned by the humanizing exploit of rigid abruptness on the counter disc and toughened worn debris. Augmentation in B_4C would consequently diminish in wear. At immense velocities, the temperature over the sliding surface increases consequent of oxidation of material and thus material relocates to transpire between the pin and contradict face leading to the creation of layer. These layers smooth the progress in accomplishing greater tribological possessions more than immense velocities.

3.2. ANN results

3.2.1. Best Validation performance of Network training for foreseeing of wear rate of TMCs

Assured and successfully prediction of the wear rate of TMCs and assorted intends of the ANN architecture are

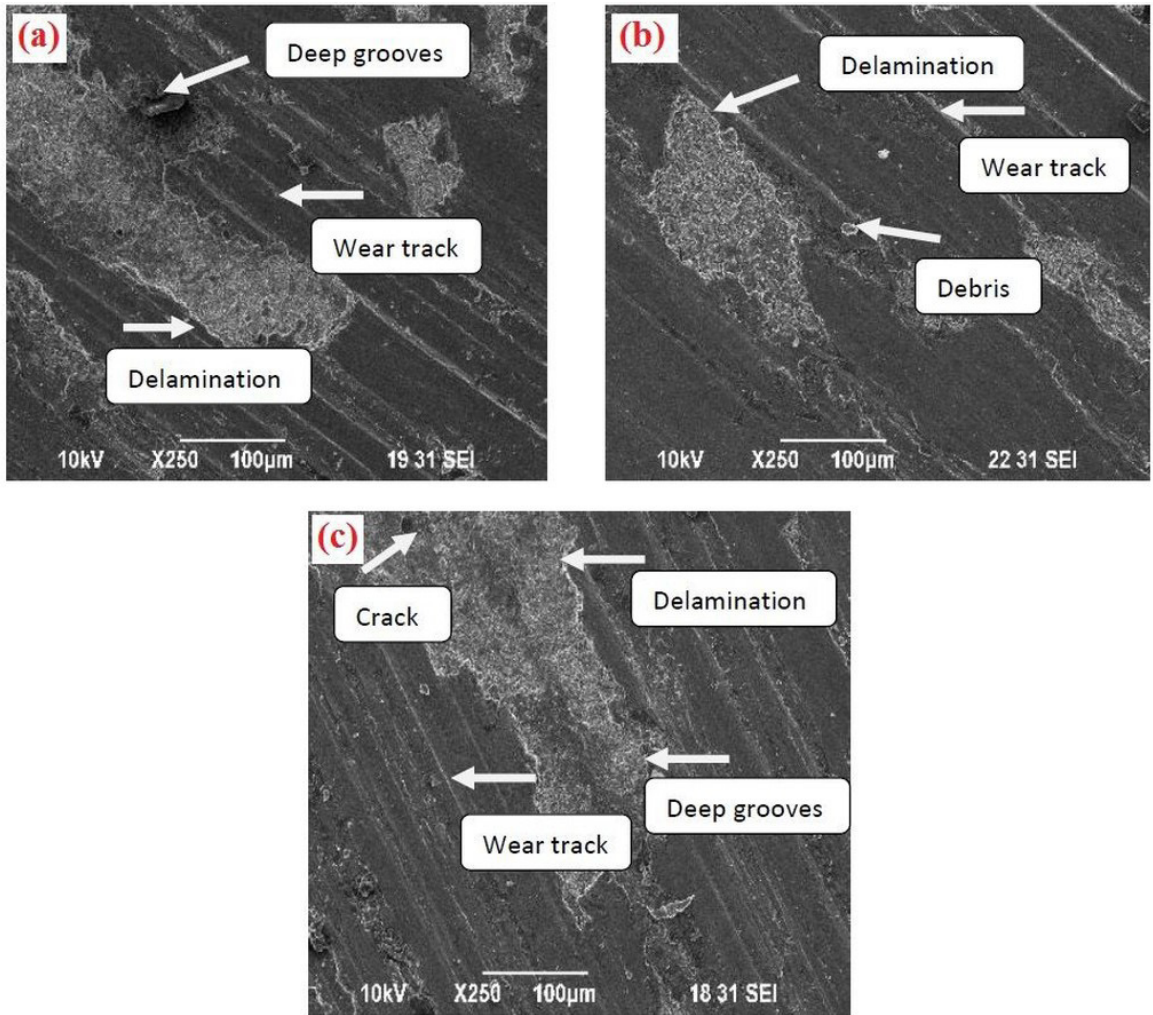


Figure 8. (a), 8(b) and 8(c) show the wear worn surfaces of the TMCs/B₄C that were studied using scanning electron microscope (SEM) for the optimal parameters at (a) 20N (b) 40N (c) 60N.

endeavoured for this kind of examination, investigating different parameters, perceptibly, is imperative in promising the most excellent and consistent ANN structure which is associated to take care of the model and its associations to the full extent for sequence developed. In this research, the single based hidden layer of 3-10-2 (input-hidden-output) ANN structure was finally decided.

The ANN structure is designed with 3 credentials suggesting the number of input parameters in that order and the complementary '10' suggests the number of neurons (hidden layer), used as an ingredient of the buried layer, at the same time and the last '2' specifies the measure of a parameter in the output. The ANN was programmed to use a Levenburg-Marquardt algorithm. MATLAB R2018b software was wont to instruct the network for innumerable periods nearly allowing 9000 epochs to accomplish an adequate recital²⁷. In this investigational process, the network was instructed for the best validation performance of WR and CoF for 2087 epochs and 3253 epochs. The recital of the ANN is finalized by MSE. Biases and weights are attuned iteratively

throughout training by taking into consideration the MSE⁵⁶⁻⁵⁸. All experimental data is reduced by MSE. Figure 9 shows MSE is abridged for the purpose of the number of epochs for best validation. The most excellent recital is acquired for WR and CoF at 2087 epochs and 3253 epochs and displaying an MSE value of 2.3939e-06 and 1.1865e-08 respectively. This minimum value shows accuracy of good prediction.

3.2.2. Correlation coefficients plots of training, testing, and validation using ANN for Wear prediction

The precision of the planned and ANN model for wear rate can be calculated significantly different from Figure 10. It is obvious that every experimental value is secure in accordance with the predicted values of the planned and ANN models. Figure 10 provides proof of the precision of the ANN evaluation by contrasting curves of best fit for training, testing, validation, and rate of wear against experimental data. The subsequent correlation coefficients were attained for training, testing, validation, and all wear rate: 0.99287, 0.99986, 0.99814, and 0.99417, respectively.

These values signify an extremely secure relationship between the experimental data and ANN model.

3.2.3. Correlation coefficients plots of training, testing, validation using ANN for COF prediction

Most suitable curves were urbanized for training, testing, and validation of the ANN used. Figure 11 gives a hint of the accurateness of the ANN assessment by contrasting curves most suitable for training, testing, validation, and CoF adjacent to experimental data. Correlation coefficients of 0.99063, 0.9982, 0.99955, and 0.9935 were obtained for the training, testing, validation, and all sets of CoF respectively.

3.2.4. Comparison of experimental, ANN and regression model

The regression and ANN models are compared with experimental results. The percentage of error is determined among the experimental results. It is perceptible that taken together the models are reliable with the experimental results. MAD, MSE, RMSE, and MAPE values imitate the intention of the ANN model which is excellent and precise as contrasted to the regression model and the values are given in Table 4 for wear rate and CoF. The results observed from the investigations are illustrated in Table 5 and its graphical representation of wear and CoF is shown in Figures 12 and 13.

Regression analysis is applied to find the rapport amid sovereign erratic and reliant variables and to predict reliable variables. In this analysis, R is of the value of the correlation coefficient and it is utilized to explain the validity of urbanized regression models. The WR of homogeneous TMCs composites following equation is given,

Regression Equation:

$$WR = -0.0181 - 0.000249L + 0.00747V + 0.000015D + 0.000005L * L - 0.000942V * V - 0.000003D * D \quad (1)$$

$$CoF = -0.01221 + 0.001244L + 0.00942V - 0.000004D - 0.000001L * L - 0.000461V * V + 0.000001D * D \quad (2)$$

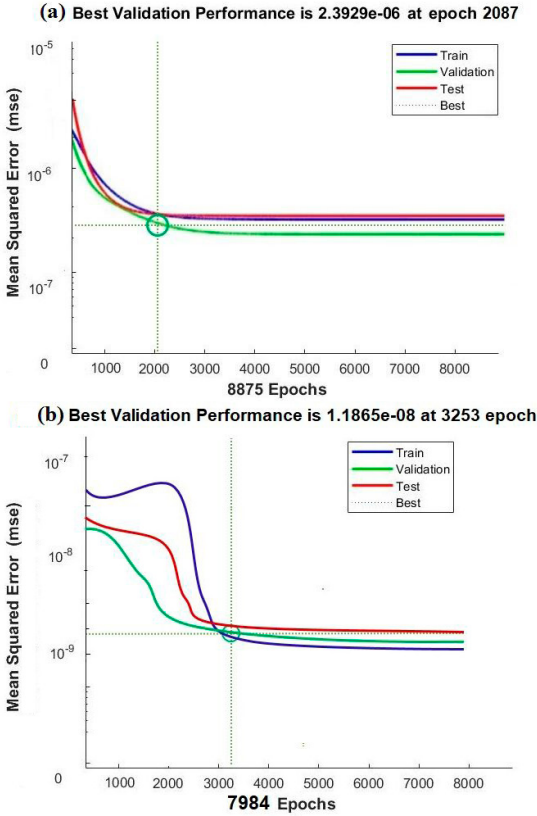


Figure 9. Network training to (a) predict WR of TMCs (b) predict CoF of TMCs.

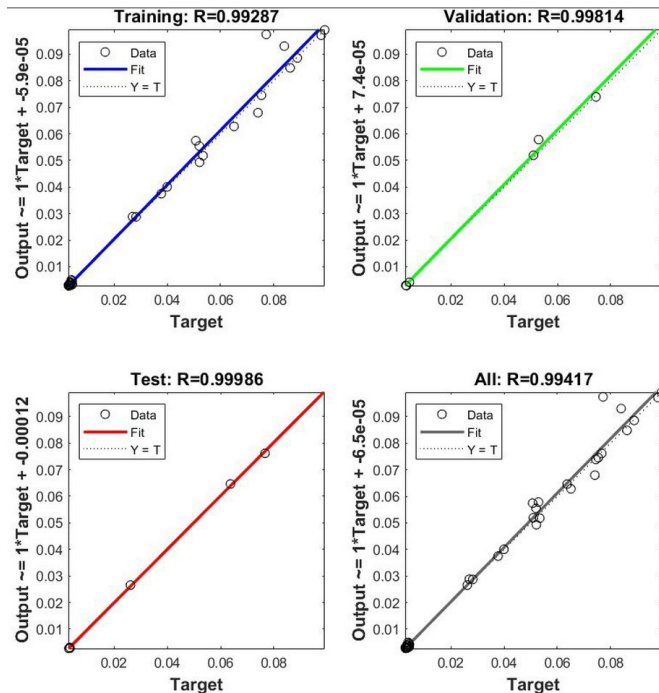


Figure 10. Line of best fit for a correlation coefficient between actual and predicted values for training, validation, testing and all wear rate data.

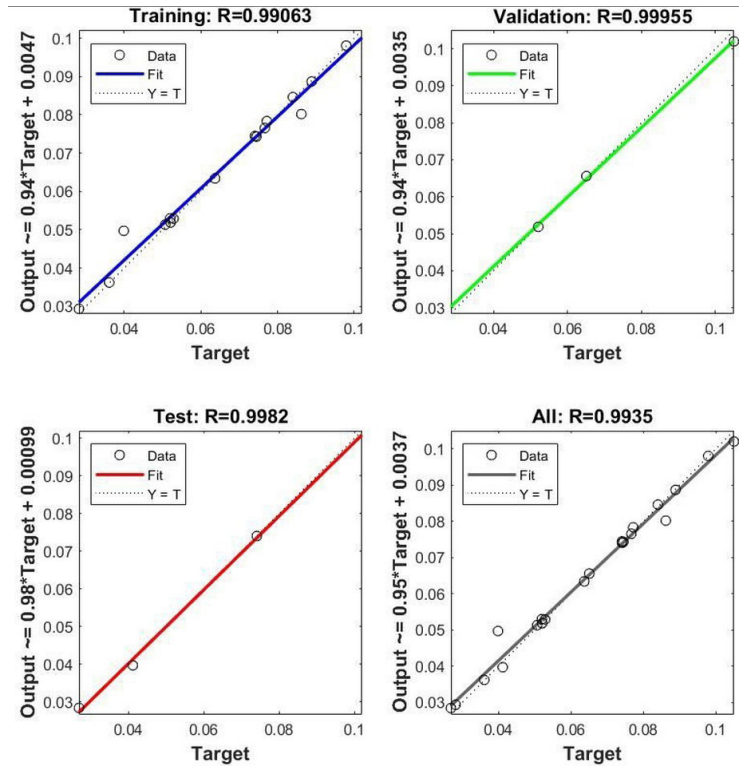


Figure 11. Correlation coefficients plots of training, testing, validation, and combination with all sets of COF using ANN for TMCs.

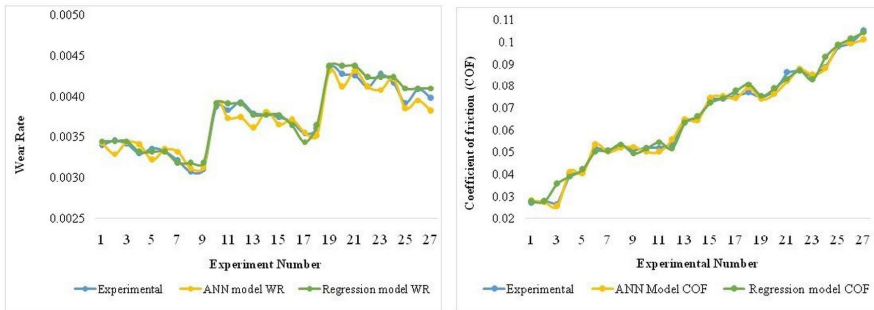


Figure 12. Graphical representation of Experimental, ANN and Regression model for wear rate and CoF.

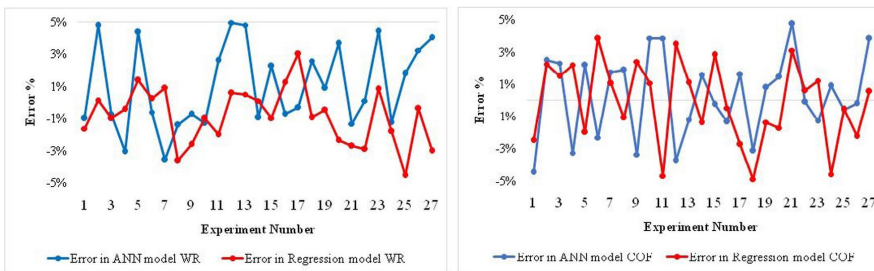


Figure 13. Graphical representation of Errors in ANN and Regression model for wear rate and CoF.

Table 4. Comparison of Regression and ANN Models.

Parameters	Regression Model				ANN Model			
	MAD	MSE	RMSE	MAPE	MAD	MSE	RMSE	MAPE
Wear Rate	5.71111E-05	5.216519E-09	7.22255E-05	1.52%	8.53852E-05	1.086810E-08	0.00010425	2.27%
CoF	0.001353407	2.81658E-06	0.001678268	2.12%	0.001285185	2.57222E-06	0.001603815	2.17%

Table 5. Comparison of Experimental, ANN and Regression models for Wear rate, CoF and Errors.

Input			Experimental Output		Predicated ANN Output				Predicated Regression Model			
L (N)	V(m/s)	D(m)	WR	CoF	WR	CoF	WR error	CoF error	WR	CoF	WR error	CoF error
20	2	1000	0.003396	0.0269	0.003429	0.0281	-0.0000330	-0.0012	0.003451	0.0276	-0.0000550	-0.000666
20	2	2000	0.003456	0.0282	0.003291	0.0275	0.0001650	0.0007	0.003451	0.0276	0.0000050	0.000634
20	2	3000	0.003417	0.0261	0.003441	0.0255	-0.0000240	0.0006	0.003451	0.0356	-0.0000340	0.000534
20	4	1000	0.003301	0.0399	0.003402	0.0412	-0.0001010	-0.0013	0.003315	0.0390	-0.0000140	0.000878
20	4	2000	0.003362	0.0412	0.003215	0.0403	0.0001470	0.0009	0.003315	0.0420	0.0000470	-0.000822
20	4	3000	0.003323	0.052	0.003343	0.0532	-0.0000200	-0.0012	0.003315	0.0500	0.0000080	0.001978
20	6	1000	0.003207	0.051	0.003321	0.0501	-0.0001140	0.0009	0.003179	0.0505	0.0000280	0.000522
20	6	2000	0.003068	0.0529	0.003111	0.0519	-0.0000430	0.001	0.003179	0.0535	-0.0000110	-0.000578
20	6	3000	0.003098	0.0507	0.003121	0.0524	-0.0000230	-0.0017	0.003179	0.0495	-0.0000810	0.001222
40	2	1000	0.003873	0.0521	0.003923	0.0501	-0.0000500	0.002	0.003911	0.0515	-0.0000380	0.000554
40	2	2000	0.003834	0.0521	0.003734	0.0501	0.0001000	0.002	0.003911	0.0545	-0.0000770	-0.002446
40	2	3000	0.003934	0.0534	0.003739	0.0554	0.0001950	-0.002	0.003911	0.0515	0.0000230	0.001854
40	4	1000	0.003794	0.0637	0.003612	0.0645	0.0001820	-0.0008	0.003775	0.0630	0.0000190	0.000698
40	4	2000	0.003779	0.0651	0.003814	0.0641	-0.0000350	0.001	0.003775	0.0660	0.0000040	-0.000902
40	4	3000	0.003739	0.0741	0.003655	0.0743	0.0000840	-0.0002	0.003775	0.0720	-0.0000360	0.002098
40	6	1000	0.003684	0.0741	0.003711	0.0751	-0.0000274	-0.001	0.003639	0.0745	0.0000450	-0.000358
40	6	2000	0.003545	0.0754	0.003557	0.0742	-0.0000120	0.0012	0.003439	0.0775	0.00001060	-0.002058
40	6	3000	0.003605	0.0767	0.003512	0.0791	0.0000930	-0.0024	0.003639	0.0805	-0.0000340	-0.003758
60	2	1000	0.004350	0.0745	0.004312	0.0739	0.0000380	0.0006	0.004371	0.0755	-0.0000210	-0.001026
60	2	2000	0.004271	0.0772	0.004114	0.0761	0.0001570	0.0011	0.004371	0.0785	-0.0001000	-0.001326
60	2	3000	0.004256	0.0862	0.004312	0.0821	-0.0000560	0.0041	0.004371	0.0835	-0.00001150	0.002674
60	4	1000	0.004116	0.0875	0.004112	0.0876	0.0000040	-0.0001	0.004235	0.0870	-0.00001190	0.000518
60	4	2000	0.004270	0.084	0.004081	0.0851	0.0001890	-0.0011	0.004235	0.0830	0.0000350	0.001018
60	4	3000	0.004161	0.0889	0.004212	0.0881	-0.0000510	0.0008	0.004235	0.0930	-0.0000740	-0.004082
60	6	1000	0.003922	0.0979	0.003852	0.0985	0.0000700	-0.0006	0.004099	0.0984	-0.00001770	-0.000538
60	6	2000	0.004083	0.0992	0.003951	0.0994	0.0001320	-0.0002	0.004099	0.1014	-0.0000160	-0.002238
60	6	3000	0.003979	0.105	0.003819	0.101	0.0001600	0.004	0.004099	0.1044	-0.00001200	0.000562

4. Conclusions

The conclusions of present investigation are as the follows:

- The TMCs/B₄C composite is prepared by the powder metallurgy route.
- The pin-on-disc wear test machine has revealed that the wear resistance increase in the midst of augmentation B₄C up to 3, 6, and 9%.
- Regression and ANN models have been effectively urbanized and reveal exceptional precision and reliability. In this research both models were compared and it is observed that the accuracy of the ANN model is better than the regression model.
- From the ANN study, the predicted data was related to investigational data and high degree of accuracy was observed and the R-value was in the assortment of 0.9 to 0.999. The error in prediction was calculated to be less than 4%. The use of ANN for prediction played a vital role.
- The excellent conformity was realized between experimental and ANN values of the output of the wear parameter.

5. References

1. Ali MH, Ansari MNM, Khidhir BA, Mohamed B, Oshkour AA. Simulation machining of titanium alloy (Ti-6Al-4V) based on the finite element modeling. *J Braz Soc Mech Sci Eng.* 2014;36(2):315-24.
2. Boyer RR. An overview on the use of titanium in the aerospace industry. *Mater Sci Eng A.* 1996;213:103-14.
3. Banerjee D, Williams JC. Perspectives on titanium science and technology. *Acta Mater.* 2013;61:844-79.
4. Leyens C, Peters M. (2006) Titanium and titanium alloys: fundamentals and applications. New York: John Wiley & Sons; 2006.
5. Gangwar K, Ramulu M. Friction stir welding of titanium alloys: a review. *Mater Des.* 2018;141:230-55.
6. Wu D, Zhang LG, Liu LB, Bai WM, Zeng LJ. Effect of Fe content on microstructures and properties of Ti-6Al-4V alloy with combinatorial approach. *Trans Nonferrous Met Soc China.* 2018;28:1714-23.
7. Dogan O, Hawk J, Tylczak J, Wilson R, Govier R. Wear of titanium carbide reinforced metal matrix composites. *Wear.* 1999;225:758-69.
8. Tjong S, Ma Z. Microstructural and mechanical characteristics of in situ metal matrix composites. *Mater Sci Eng Rep.* 2000;29:49-113.
9. Tan MJ, Chen GW, Thiruvarduchelvan S. High temperature deformation in Ti-5Al-2.5Sn alloy. *J Mater Process Technol.* 2007;192:434-8.
10. Wei K, Wang Z, Zeng X. Preliminary investigation on selective laser melting of Ti-5Al-2.5Sn Ti alloy: from single tracks to bulk 3D components. *J Mater Process Technol.* 2017;244:73-85.
11. Jiao Y, Huang L, Geng L. Progress on discontinuously reinforced titanium matrix composites. *J Alloys Compd.* 2018;767:1196-215.
12. Junaid M, Khan FN, Bakhsh N, Baig MN, Rahman K. Study of microstructure, mechanical properties and residual stresses in full penetration electron beam welded Ti-5Al-2.5Sn alloy sheet. *Mater Des.* 2018;139:198-211.

13. Sun QY, Gu HC. Tensile and low-cycle fatigue behavior of commercially pure titanium and Ti–5Al–2.5Sn alloy at 293 and 77K. *Mater Sci Eng A*. 2001;316:80-6.
14. Sun QY, Song SJ, Zhu RH, Gu HC. Toughening of titanium alloys by twinning and martensite transformation. *J Mater Sci*. 2002;37:2543-7.
15. Canakci A. Microstructure and abrasive wear behaviour of B₄C particle reinforced 2014 Al matrix composites. *J Mater Sci*. 2011;46(8):805-13.
16. Ramesh CS, Keshavamurthy R, Channabasappa BH, Pramod S. Friction and wear behavior of Ni–P coated Si₃N₄ reinforced Al6061 composites. *Tribol Int*. 2010;43(3):623-34.
17. Choi B, Kim Y. In-Situ (TiB+TiC) particulate reinforced titanium matrix composites: effect of B₄C size and content. *Met Mater Int*. 2013;19:1301-7.
18. Jia L, Li SF, Imai H, Chen B, Kondoh K. Size effect of B₄C powders on metallurgical reaction and resulting tensile properties of Ti matrix composites by in-situ reaction from Ti–B₄C system under a relatively low temperature. *Mater Sci Eng A*. 2018;614:129-35.
19. Ramkumar T, Narayanasamy P, Selvakumar M, Balasundar P. Effect of B₄C reinforcement on the dry sliding wear behaviour of Ti–6Al–4V/B₄C sintered composites using response surface methodology. *Arch Metall Mater*. 2018;63(3):1179-200.
20. Xue B, Yunxue J, Xuan L, Yanan C. Friction and wear performance of in-situ (TiC+TiB)/Ti6Al4V composites. *Rare Met Mater Eng*. 2018;12(12):3624-8.
21. Prakash KS, Moorthy RS, Gopal PM, Kavimani V. Effect of reinforcement, compact pressure and hard ceramic coating on aluminium rock dust composite performance. *Int J Refract Met Hard Mater*. 2015;54:223-9.
22. Pal S, Pal SK, Samantaray AK. Artificial neural network modeling of weld joint strength prediction of a pulsed metal inert gas welding process using arc signals. *J Mater Process Technol*. 2008;202:464-74.
23. Hayajneh M, Hassan AM, Alrashdan A, Mayyas AT. Prediction of tribological behavior of aluminium–copper based composite using artificial neural network. *J Alloys Compd*. 2009;470:584-8.
24. Xiao G, Zhu Z. Friction materials development by using DOE/RSM and artificial neural network. *Tribol Int*. 2010;43:218-27.
25. Zhang Z, Friedrich K, Velten K. Prediction on tribological properties of short fibre composites using artificial neural networks. *Wear*. 2002;252:668-75.
26. Abidoeye LK, Mahdi FM, Idris MO, Alabi OO, Wahab AA. ANN-derived equation and ITS application in the prediction of dielectric properties of pure and impure CO₂. *J Clean Prod*. 2018;175:123-32.
27. Palanivel R, Laubscher RF, Dinaharan I, Murugan N. Tensile strength prediction of dissimilar friction stir-welded AA6351–AA5083 using artificial neural network technique. *J Braz Soc Mech Sci Eng*. 2016;38:1647-57.
28. Shakeri S, Ghassemi A, Hassani M, Hajian A. Investigation of material removal rate and surface roughness in wire electrical discharge machining process for cementation alloy steel using artificial neural network. *Int J Adv Manuf Technol*. 2015;82:549-57.
29. Karazi SM, Issaand A, Brabazon D. Comparison of ANN and DoE for the prediction of laser-machined micro-channel dimensions. *Opt Lasers Eng*. 2009;47:956-64.
30. Mondal N, Mandal S, Mandal MC. FPA based optimization of drilling burr using regression analysis and ANN model. *Measurement*. 2020;152:107327.
31. Hassan AKF, Mohammed LS, Abdulsamad HJ. Experimental and artificial neural network ANN investigation of bending fatigue behavior of glass fiber/ polyester composite shafts. *J Braz Soc Mech Sci Eng*. 2018;40(4):2-10.
32. Ashan SK, Ziaiefar N, Khalilnezhad R. Artificial neural network modelling of Cr (VI) surface adsorption with NiO nanoparticles using the results obtained from optimization of response surface methodology. *Neural Comput Appl*. 2018;29(10):969-79.
33. Chen Y, Sun R, Gao Y, Leopold J. A nested-ANN prediction model for surface roughness considering the effects of cutting forces and tool vibrations. *Measurement*. 2017;98:25-34.
34. Wang ZH, Gong DY, Li X, Li GT, Zhang DH. Prediction of bending force in the hot strip rolling process using Artificial Neural Network and Genetic Algorithm (ANN-GA). *Int J Adv Manuf Technol*. 2017;93:3325-38.
35. Aydin G, Karakurt I, Hamzacebi C. Artificial neural network and regression models for performance prediction of abrasive water jet in rock cutting. *Int J Adv Manuf Technol*. 2014;75:1321-30.
36. Argatov II, Chai YS. An artificial neural network supported regression model for wear rate. *Tribol Int*. 2019;138:211-4.
37. Palanivel R, Dinaharan I, Laubscher RF. Application of an artificial neural network model to predict the ultimate tensile strength of friction welded titanium tubes. *J Braz Soc Mech Sci Eng*. 2019;41:1-13.
38. Kucukoglu I, Atici-Ulusu H, Gunduz T, Tokcalar O. Application of the artificial neural network method to detect defective assembling processes by using a wearable technology. *J Manuf Syst*. 2018;49:163-71.
39. Baig RU, Javed S, Kazi A, Quyam M. Artificial neural network approach for the prediction of wear for Al6061 with reinforcements. *Mater Res Express*. 2020;7:1-17.
40. Sosimi AA, Gbenedor OP, Oyerinde O, Bakare OO, Adeosun SO, Olaleye SA. Analysing wear behaviour of Al–CaCO₃ composites using ANN and sugeno-type fuzzy inference systems. *Neural Comput Appl*. 2020;32:13453-64.
41. Mutuk T, Gürbüz M, Mutuk H. Prediction of wear properties of graphene-Si₃N₄ reinforced titanium hybrid composites by artificial neural network. *Mater Res Express*. 2020;7:1-10.
42. Kannaiyan M, Raghuvaran JGT. Prediction of specific wear rate for LM25/ZrO₂ composites using Levenberg–Marquardt back propagation algorithm. *J Mater Res Technol*. 2020;9:530-8.
43. Dinaharan I, Palanivel R, Murugan N, Laubscher RF. Application of artificial neural network in predicting the wear rate of copper surface composites produced using friction stir processing. *Aust J Mech Eng*. 2020;18:1-12.
44. Pati PR. Prediction and wear performance of red brick dust filled glass–epoxy composites using neural networks. *International Journal of Plastics Technology*. 2019;23:253-60.
45. Megahed M, Saber D, Agwa MA. Modeling of wear behavior of Al–Si/Al₂O₃ metal matrix composites. *Phys Met Metallogr*. 2019;120(10):981-8.
46. Mahanta S, Chandrasekaran M, Samanta S, Arunachalam R. Multi-response ANN modelling and analysis on sliding wear behaviour of Al7075/B₄C/fly ash hybrid nanocomposites. *Mater Res Express*. 2019;6:1-18.
47. Pramod R, Veeresh Kumar GB, Shivakumar Gouda PS. A study on the Al₂O₃ reinforced Al7075 metal matrix composites wear behavior using artificial neural networks. *Mater Today Proc*. 2018;5(5):11376-85.
48. Satyanarayana G, Naidu GS, Hari Babu N. Artificial neural network and regression modelling to study the effect of reinforcement and deformation on volumetric wear of red mud nanoparticles reinforced aluminium matrix composites synthesized by stir casting. *Bol Soc Esp Ceram Vidr*. 2018;57:91-100.
49. Hanief M, Wani MF. Modeling and prediction of surface roughness for running-in wear using Gauss-Newton algorithm and ANN. *Appl Surf Sci*. 2015;357:1573-7.
50. Ghisi A, Mariani S. Mechanical characterization of Ti–5Al–2.5Sn ELI alloy at cryogenic and room temperatures. *Int J Fract*. 2007;146:61-77.
51. Zeng X, Liu W, Xu B, Shu G, Li Q. Microstructure and Mechanical Properties of Al–SiC nanocomposites synthesized by surface-modified aluminium powder. *Metals (Basel)*. 2018;8(4):1-11.

52. Prajapati DK, Tiwari M. Use of artificial neural network (ANN) to determining surface parameters, friction and wear during pin-on-disc tribo testing. *Key Eng Mater.* 2017;739:87-95.
53. Karthickeyan V, Balamurugan P, Rohith G, Senthil R. Developing of ANN model for prediction of performance and emission characteristics of VCR engine with orange oil biodiesel blends. *J Braz Soc Mech Sci Eng.* 2017;39(7):2877-88.
54. Samet G, Unver B, Altin I. Prediction of cyclic variability in a diesel engine fueled with n-butanol and diesel fuel blends using artificial neural network. *Renew Energy.* 2018;117:538-44.
55. Charudatta Kshirsagar M, Ramanathan A (2017). Artificial neural network applied forecast on a parametric study of *Calophyllum Inophyllum* methyl ester diesel engine out responses. *Appl Energy* 189:555-567. <https://doi.org/10.1016/j.apenergy.2016.12.045>.
56. Kshirsagar CM, Anand R. Artificial neural network applied forecast on a parametric study of *Calophyllum Inophyllum* methyl ester diesel engine out responses. *Appl Energy.* 2017;189:555-67.
57. Soundararajan R, Ramesh A, Sivasankaran S, Vignesh M. Modeling and analysis of mechanical properties of aluminium alloy (A413) reinforced with boron carbide (B_4C) processed through squeeze casting process using artificial neural network model and statistical technique. *Mater Today Proc.* 2017;4(2):2008-30.
58. Soundararajan R, Ramesh A, Sivasankaran S, Sathishkumar A. Modeling and analysis of mechanical properties of aluminium alloy (A413) processed through squeeze casting route using artificial neural network model and statistical technique. *Adv Mater Sci Eng.* 2015;2015:1-16.